Tolerance on sphere radius for the calibration of the transfer function of coherence scanning interferometry

Rong Su*[a], Jeremy M. Coupland[b], Yuhang Wang[c], Richard K. Leach[a]

[a]Manufacturing Metrology Team, Faculty of Engineering, The University of Nottingham, University Park, Nottingham NG7 2RD, UK; [b]Wolfson School of Mechanical, Electrical and Manufacturing Engineering, Loughborough University, Loughborough LE11 3TU, UK; [c]Ultra-Precision Optoelectronic Instrument Engineering Centre, Harbin Institute of Technology, 92 West Da-Zhi Street, Harbin 150001, China

ABSTRACT

Although coherence scanning interferometry (CSI) commonly achieves a sub-nanometre noise level in surface topography measurement, the absolute accuracy is difficult to determine when measuring a surface that contains varying local slope angles and curvatures. Recent research has shown that it is possible to use a single sphere with a radius much greater than the source wavelength to calibrate the three-dimensional transfer function of a CSI system. A major requirement is the accurate knowledge of the sphere radius, but the three-dimensional measurement of a sphere with nanometre level uncertainty is a highly challenging metrology problem, and is not currently feasible. Perfect spheres do not exist and every measurement has uncertainty. Without having a quantitative understanding of the tolerance of the sphere radius, the calibration method cannot be used confidently for calibration of the transfer function of a CSI system that may be used in research laboratories or industry. In this paper, the effects of the tolerance of the radius of the calibration sphere on surface topography measurements are quantitatively analysed through a computational approach. CSI measurements of spherical, sinusoidal and rough surfaces are investigated in the presence of various degrees of radius error. A lookup table that relates the surface height error as a function of the radius error and surface slope angle is provided. The users may estimate the required tolerances of the sphere radius for their specific surface measurements if this calibration approach is used. The output of this paper provides a feasibility analysis for this calibration method for further development and applications.

Keywords: Transfer function, calibration, coherence scanning interferometry, tolerance, surface topography, metrology

* rong.su@nottingham.ac.uk; phone +44 1157486230; www.nottingham.ac.uk/research/manufacturing-metrology

1. INTRODUCTION

Coherence scanning interferometry (CSI) has been widely employed in the research and manufacturing environments for conducting surface topography measurement and dimensional micrometrology[1]. CSI, also known as scanning white light interferometry, encodes surface height information into the phase of the interference signal generated from a broadband source[2,3], and the surface height is calculated using a reconstruction algorithm, e.g. the frequency domain analysis (FDA)[3] or envelope detection method[4]. The precision of modern CSI systems may achieve the sub-nanometre level[5], but the absolute measurement uncertainty can be as high as tens or even hundreds of nanometres due to optical aberrations, signal processing errors and the complex geometrical form of a surface that contains varying local slope angle and curvature[6-8]. In the presence of tilt and curvature dependent errors, traditional step artefacts that contain two parallel flat surfaces are not sufficient for calibration of CSI systems[9].

A recent theoretical study[10,11] showed that the surface measurement by a CSI system can be considered as a 3D linear filtering operation on the basis of scalar diffraction theory. For the so-called "foil model" of a surface to be valid, the Kirchhoff approximation is assumed, i.e. that the surface is slowly varying at the optical scale[12]. Within this validity regime, the CSI signal is linearly related to the object function that is determined by the surface topography and optical properties of the object. The 3D linear filtering process can be characterised by the transfer function (TF) of a CSI system. The TF contains the information on the bandwidth of the measuring system in the spatial frequency domain, and

the Fourier transform of the TF provides the point spread function of system in 3D. It has been shown that the TF can be calibrated by using a precision sphere with a diameter of approximately 50 μm[13], assuming that the sphere has good sphericity and the radius of the sphere is accurately determined. A recent paper presented a critical analysis of the calibration process, and computationally investigated the effect of measurement noise and the radius error of the calibration sphere, and demonstrated the tilt and curvature dependent errors in CSI[14].

Errors in in the calibration of CSI using the foil model can occur due to the presence of the radius error or the geometrical form error of the sphere. In addition, the three-dimensional measurement of a sphere with nanometre level uncertainty is a highly challenging metrology problem, and is not currently feasible. Thus, without having a quantitative understanding of the tolerance of the sphere radius, the calibration method cannot be used confidently for calibration of the transfer function of a CSI system. In this paper, the theoretical tolerance of the radius of the calibration sphere on surface topography measurements will be quantitatively examined.

2. PRINCIPLE

CSI is a well-established technique and its detailed principle can be found elsewhere[2,3]. The process of surface measurement using CSI can be considered as a 3D linear shift-invariant filtering operation[10,11]. This assumption is valid for strongly scattering surfaces if the foil model of the surface is applied and the Kirchhoff approximation is assumed. Within the validity regime, the TF of a CSI system H($\mathbf{k}$) can be obtained as the quotient of the CSI signal in the 3D spatial frequency domain ($\mathbf{k}$-space) F($\mathbf{k}$) and the object function O($\mathbf{k}$)

$$H(\mathbf{k}) = \frac{F(\mathbf{k})}{O(\mathbf{k})} . \tag{1}$$

F($\mathbf{k}$) can be calculated from the Fourier transform of the interference signal, and O($\mathbf{k}$) can be calculated from the Fourier transform of the object function in the spatial domain o(x,y,z), which is defined as[11]

$$o(x, y, z) = 4\pi j R w(x, y) \delta\left[z - s(x, y)\right], \tag{2}$$

where $j = \sqrt{-1}$, R is the Fresnel reflection coefficient and is assumed to be constant for simplicity[11], $w(x,y)$ is a window function that correlates with the apodization function of the imaging system, and the object is defined as an infinitely thin foil by the Dirac delta function $\delta(x,y)$ based on the surface topography of the object $s(x,y)$.

Once the TF has been measured, an inverse filter can be calculated. The primary purpose of the inverse filter is to remove the distortions in the phase term of the TF which would be constant or zero for an ideal system. The inverse filter is expressed as exp[$-j\theta(\mathbf{k})$], where $\theta(\mathbf{k})$ is the measured phase transfer function (PTF)[14].

It should be noted that the accuracy of the inverse filter and the measured PTF is dependent on the object function o(x,y,z), and particularly on the surface topography of the object $s(x,y)$. Therefore, it is critical to know the sphericity and radius of the calibration sphere to a high level of accuracy. Usually, the sphericity is qualitatively examined under an optical or electron microscope. The sphericity errors that are asymmetrical about the vertical axis of a CSI system can be easily identified (see Figure 1(a)) by looking from the top. The symmetrical errors (see Figure 1(b)) can be effectively equivalent to the radius error (see Figure 1(c)) within a certain degree of surface slope. However, the measurement of sphere radius remains a highly challenging metrology problem if accuracy is required at the nanometre level. Therefore, we will focus on the tolerance of the radius of the calibration sphere in this study.
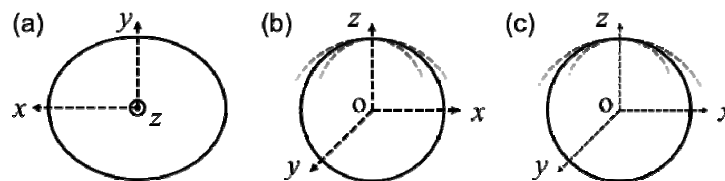

Figure 1. Schema of geometrical errors of a sphere: a) asymmetrical and b) symmetrical form error; c) radius error.

3. METHOD

3.1 Calibration and inverse filtering

The effect and tolerances of the radius of the calibration sphere are investigated here through a computational approach. The simulated CSI system is aberration-free, such that the nominal PTF of the simulated CSI system is zero, and is assumed to be shift-invariant. The distortion of the PTF after a miscalibration is shown as a phase deviation from zero. The calibration and inverse filtering processes are illustrated in Figure 2, and more details may be found elsewhere[14]. In general, to study the effects of the radius error, we first simulate the fringe data of a nominal sphere with a known radius R_0 in a CSI system with a certain numerical aperture (NA) and given source spectrum. The simulated fringe data is effectively equivalent to that which can be obtained from an experimental CSI measurement. The TF can be measured using a simulated calibration sphere with radius R_C and radius error $\Delta R_0 = R_C - R_0$. Errors in the measured TF will be present when $\Delta R_0 \neq 0$. After calibration of the TF, the inverse filter is calculated. The inverse filter can be applied to the measurements of different surfaces using the same CSI system.
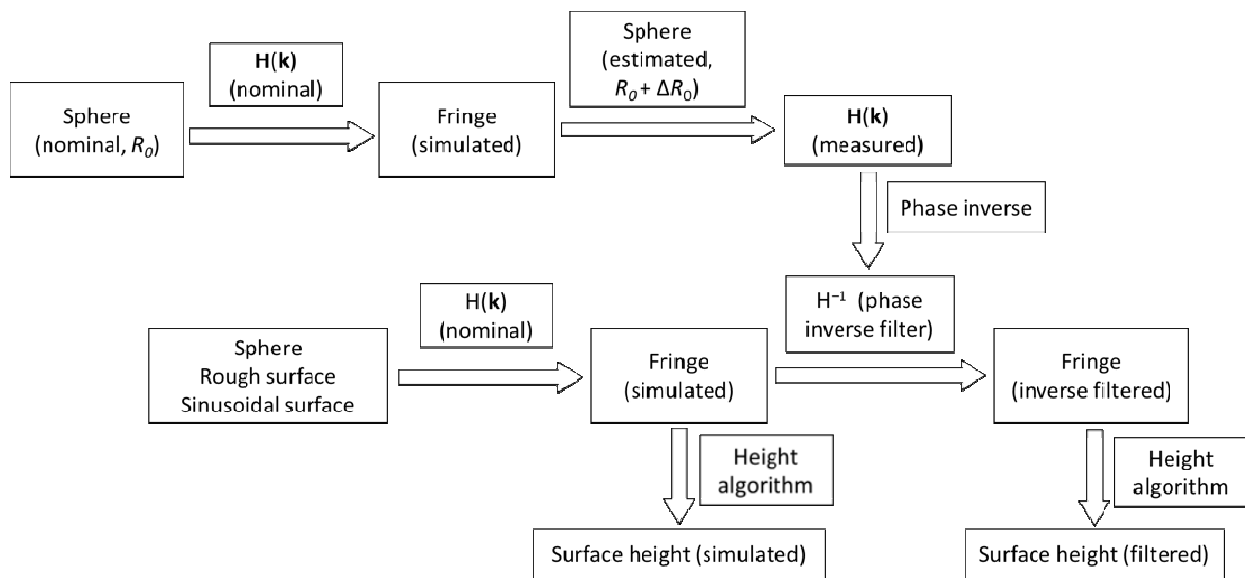

Figure 2. Flowchart of the signal modelling, TF calibration and inverse filtering process.

If the calibration is correctly and accurately carried out, i.e. the sphere form error is sufficiently small to be neglected, the optical aberrations, if present in the system, will be captured in the PTF. In such cases, the inverse filtering will improve the measurement by compensating for the errors caused by the aberrations. If the calibration is carried out in the presence of radius error, although the error caused by aberrations may still be compensated, an additional error may occur. This additional error should be supressed as much as possible by reducing ΔR_0. Given a tolerance of a surface topography measurement, what is the maximum ΔR_0 that can be tolerated? This question will be answered in this paper.

3.2 Measurement error analysis

In this study, sphere surfaces and engineering surfaces with planar and sinusoidal forms will be simulated (see Figure 2). Surface roughness is added to the planar surface, and is generated with a given root-mean-square (RMS) roughness value δ_{RMS} and an appropriate power spectrum density (PSD) function. The sinusoidal surface is described by a sine function with a period λ_G and amplitude A_G.

The surface height is calculated from the fringe data using the frequency domain analysis (FDA) method based on phase evaluation[3]. The simulated and the inverse filtered surface will be compared with the nominal surface height for obtaining the deterministic differences.

4. RESULTS

4.1 Effect of the radius error

The simulated CSI system has a NA of 0.55, central wavelength $\lambda_0 = 0.58$ μm and spectrum width $\Delta\lambda = 0.08$ μm (full-width at half maximum value). The simulated sphere has a nominal radius $R_0 = 40$ μm and a radius error $\Delta R_0 = 1$ μm. The nominal TF is shown in Figure 3(a) and Figure 3(b), and the miscalibrated TF is shown in Figure 3(c) and Figure 3(d). The MTFs are nearly identical, but the distortion in the miscalibrated PTF is pronounced, as the phase value should be zero within the system passband. The distortion is especially strong in the high spatial frequency regions along the k_x axis, and will be propagated to the phase inverse filter. When the incorrect phase inverse filter is applied to the measured fringe data, measurement error of surface height will occur and be dependent on the degree of distortion. The error is in addition to the measurement errors that already exist in the CSI system.
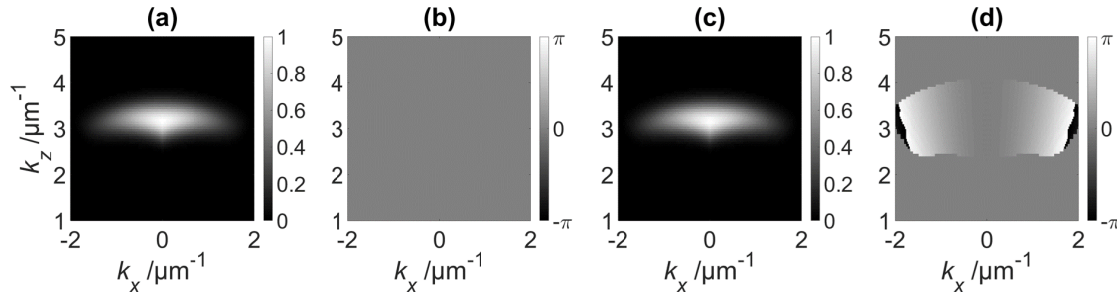

Figure 3. The nominal MTF (a) and PTF (b), and the miscalibrated MTF (c) and PTF (d) with the nominal radius $R_0 = 40$ μm and a radius error $\Delta R_0 = 1$ μm. The 2D cross-sectional views through planes $k_y = 0$ of the TFs are used for display purposes.

The additional surface height error for measuring a sphere is plotted in Figure 4 as a function of ΔR_0 and the difference of the surface slope angle from 0°. It can be seen that the height error due to miscalibration is almost proportional to the radius error at all slope angles other than 0°. The error increases rapidly at high slope angles, and can only be observed when a surface containing slope variations is measured, i.e. this tilt dependent error cannot be observed if a flat and smooth surface is measured because in that case the error results in a constant axial shift of the entire surface. However, when a sphere is measured, which contains a continuous change of surface tilt, the error introduced by the miscalibration will cause an incorrect measurement of the spherical cap. For example, miscalibration with 1 μm radius error will cause a height error of approximately 160 nm at 30° surface slope.
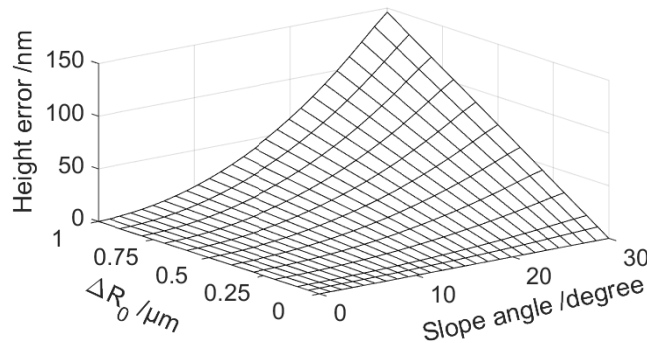

Figure 4. Height measurement error as a function of ΔR_0 and the surface slope angle.

4.2 Tolerance of the sphere radius on surface measurement

We have shown that additional height errors will be caused by the miscalibration using a sphere with radius error. The tolerance on sphere measurement can be easily derived from Figure 4. In this section, two rough surfaces with $\delta_{RMS} = 0.05$ μm and 0.1 μm, respectively, are simulated. The effect of the miscalibration ($\Delta R_0 = 1$ μm) on measurements of rough surfaces is shown in Figure 5 and the result is given in Table 1. It is noted that tilt and curvature dependent errors may occur even in an aberration-free CSI system due to the limited lateral imaging bandwidth of the system[14]. These

errors may be reduced by correctly calibrating the TF and flattening the MTF (see reference [14] for more details). If the calibration is conducted incorrectly using a sphere with radius error, the additional height error will occur and is correlated with the width of the distribution of the surface slopes. It is possible to estimate the additional height error using the information in Figure 4, given that the surface slope distribution and the radius error of the calibration sphere are known.
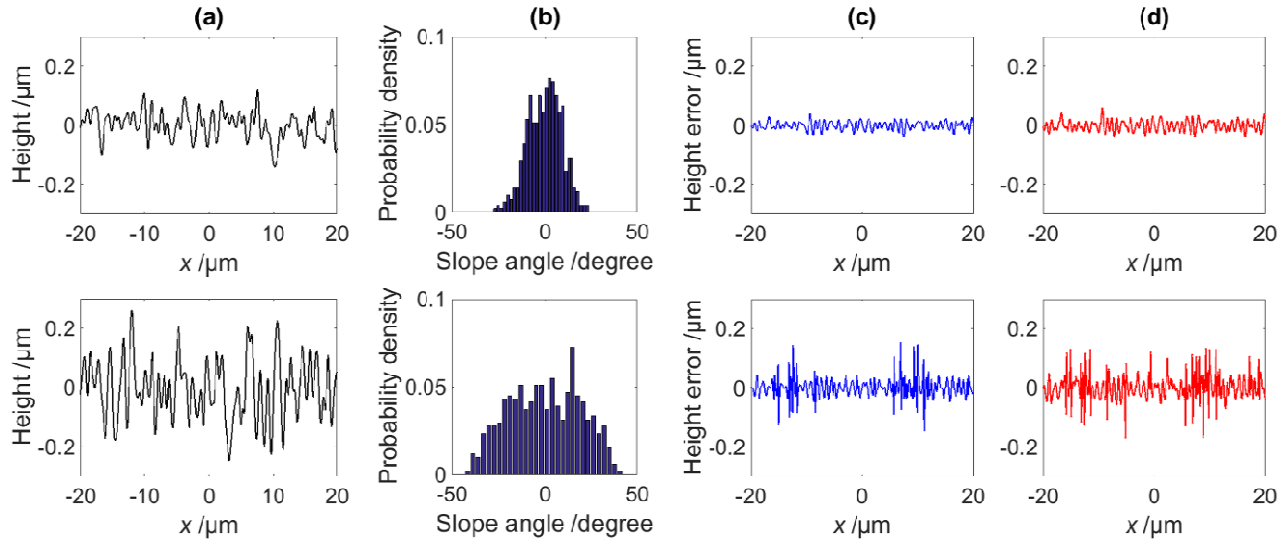

Figure 5. Height error estimation for flat surfaces with δ_{RMS} = 0.05 µm (upper) and 0.1 µm (lower). a) Surface profiles; b) distribution of local slope angle; c) height difference between the simulated and the nominal surface; d) height difference between the inverse filtered and the nominal surface (at ΔR_0 = 1 µm). The 2D cross-sectional views through planes y = 0 of the surfaces are used for display purposes.

Table 1 Sinusoidal surfaces parameters

Surfaces	δ_{RMS} / µm	Slope distribution (RMS width) /degree	Original height error (RMS) / µm	Height error after inverse filtering (RMS) / µm
R1	0.05	9	0.013	0.017
R2	0.1	19	0.035	0.043

In practice, it is possible to measure the sphere radius with an accuracy of better than 1 µm using a micro-coordinate measurement machine[15]. Alternatively, the sphere can be placed on a clean and smooth flat surface and the diameter is measured as the distance between the top of the sphere and the flat surface using a CSI or confocal microscope, but the sphericity is difficult to determine.

Another example shows the simulations of the CSI measurements of sinusoidal surfaces of which the periods and amplitudes are given in Table 2. Sinusoidal surfaces provide a generality as the topographic function of most surfaces can be approximated as a superposition of a series of sinusoidal functions with different amplitudes and periods.

Table 2 Sinusoidal surfaces parameters

Surfaces	a	b	c
λ_G /µm	10	10	5
A_G /µm	0.5	0.25	0.25

The profiles and the height errors of the three surfaces are shown in Figure 6. In the case of an aberration-free CSI the original measurement errors for the sinusoidal surfaces are mainly curvature dependent (solid blue curves), whereas the additional height errors due to miscalibration (with $\Delta R_0 = 1$ μm) are tilt dependent (dashed red curves). Both types of errors are smaller for surface (b) as this surface has the smallest surface tilt and radius of curvature at the peaks and valleys of the sinusoidal surface. In general, the errors result in a reduced amplitude of the measured sinusoidal surface[8,14,16]. This effect may also be considered as a result of the limited optical resolution determined by the NA. The additional height errors due to miscalibration are plotted in the solid curves.
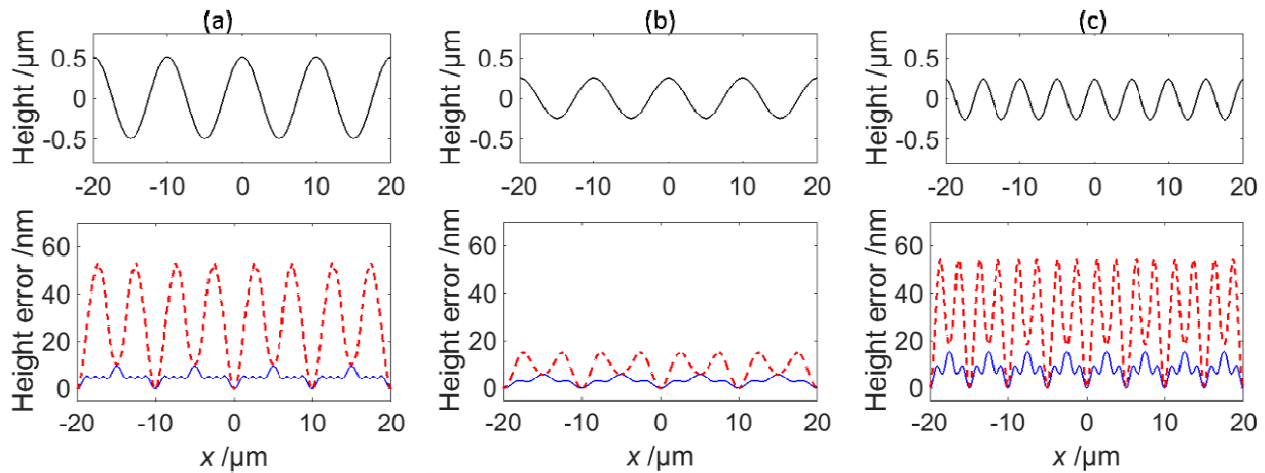

Figure 6. Profiles and height errors of CSI measurements of sinusoidal surfaces. The nominal profiles are shown in the first row. The original measurement errors and the additional height errors due to the miscalibration ($\Delta R_0 = 1$ μm) are shown in the solid blue curves and dashed red curves, respectively. The 2D cross-sectional views through planes $y = 0$ of the surfaces are used for display purposes.

The additional height errors due to the miscalibration using a sphere with a radius error $\Delta R_0 = 1$ μm are of the order of a few tens of nanometres for the example sinusoidal surfaces. The magnitude of this error is strongly correlated with the amplitude and period of the sinusoidal surface. The largest error occurs at the highest surface slope. The tolerance can be estimated from the information provided in Figure 4.

5. CONCLUSIONS

In this paper, the tolerances of the calibration sphere on CSI measurements of different surfaces are investigated. The knowledge is essential for understanding the validity conditions of the calibration method for CSI systems based on the linear theory of surface measurement and the foil model of the surface.

It has been found that calibration using a sphere with 1 μm radius error will cause an additional height error of approximately 160 nm at 30º surface slope, approximately 10 nm (RMS value) for a surface with RMS roughness of 0.1 μm, and a few tens of nanometres for a sinusoidal surface with a period of 10 μm and an amplitude of 0.5 μm. We also found that the additional error, due to the radius error of the calibration sphere, is tilt dependent. The calibration method may still improve the accuracy of the CSI measurement if the effect of the miscalibration is smaller than the effect of the other systematic error sources in the system, e.g. optical aberrations.

In future work, we will continue our hunt for high precision micro-spheres with good sphericity and techniques that can measure the size and sphericity of a micro-sphere with nanometre level accuracy.

REFERENCES

[1] Piano, S., Su, R. and Leach, R. K., "Micro-scale geometry measurement," [Micro-Manufacturing Technologies and Their Applications], Springer, Switzerland, 197-221 (2017).

[2] De Groot, P., "Coherence scanning interferometry," [Optical measurement of surface topography], Springer, Berlin, 187-208 (2011).

[3] De Groot, P., "Principles of interference microscopy for the measurement of surface topography," Adv. Opt. Photon.7, 1-65 (2015).

[4] Larkin, K. G., "Efficient nonlinear algorithm for envelope detection in white light interferometry," J. Opt. Soc. Am. A 13(4), 832–843 (1996).

[5] De Groot, P., "The meaning and measure of vertical resolution in optical surface topography measurement," Appl. Sci. 7, 54-59 (2017).

[6] Gao, F., Leach, R. K., Petzing, J. and Coupland, J. M., "Surface measurement errors using commercial scanning white light interferometers," Meas. Sci. Technol. 19, 015303 (2008).

[7] Liu, M., Cheung, C. F., Ren, M. and Cheng, C. H., "Estimation of measurement uncertainty caused by surface gradient for a white light interferometer," Appl. Opt. 54, 8670-8677 (2015).

[8] Lehmann, P., "Vertical scanning white-light interference microscopy on curved microstructures," Opt. Lett. 35(11), 1768–1770 (2010).

[9] Leach, R. K., "Is one step height enough?" Proc. 30th Annual Meeting of American Society for Precision Engineering, (Austin, USA), 110–113 (2015).

[10] Coupland, J. M. and Lobera, J., "Holography, tomography and 3D microscopy as linear filtering operations," Meas. Sci. Technol. 19, 07010 (2008).

[11] Coupland, J. M., Mandal, R., Palodhi, K. and Leach, R. K., "Coherence scanning interferometry: linear theory of surface measurement," Appl. Opt. 52, 3662-3670 (2013).

[12] Born, M. and Wolf, E., [Principles of optics: electromagnetic theory of propagation, interference and diffraction of light, 7th ed.], Cambridge University Press, Cambridge, 695–734 (1999).

[13] Mandal, R., Coupland, J. M., Leach, R. and Mansfield, D., "Coherence scanning interferometry: measurement and correction of three-dimensional transfer and point-spread characteristics," Appl. Opt. 53, 1554-1563 (2014).

[14] Su, R., Wang, Y., Coupland, J. M. and Leach, R. K., "On tilt and curvature dependent errors and the calibration of coherence scanning interferometry," Opt. Express 25, 3297-3310 (2017).

[15] Küng, A., Meli, F. and Thalmann, R., "Ultraprecision micro-CMM using a low force 3D touch probe," Meas. Sci. Technol., 18, 319 (2007).

[16] Xie, W., Lehmann, P. and Niehues, J., "Lateral resolution and transfer characteristics of vertical scanning white-light interferometers," Appl. Opt. 51, 1795-1803 (2012).